Science and Technology Indonesia
e-ISSN:2580-4391 *p*-ISSN:2580-4405
Vol. 9, No. 1, January 2024

Research Paper

Palm Oil Fuel Ash and Fly Ash for a Partial Replacement of Cement in High-Quality, Environmentally Friendly Mortar as a Solution to Industrial Waste

Shinta Marito Siregar[1,2], Syahrul Humaidi[1*], Nurdin Bukit[3], Erna Frida[1]

[1]*Doctoral Program (Physics), FMIPA, Universitas Sumatera Utara, Jln Bioteknologi No 1, Medan, 20155, Indonesia*
[2]*Universitas Muslim Nusantara Al Washliyah, Jl. Garu II A No. 93, Medan, 20147, Indonesia*
[3]*Department of Physics, Universitas Negeri Medan, Jl. Willem Iskandar Pasar V, Medan, 20221, Indonesia*
***Corresponding author**: syahrul1@usu.ac.id

Abstract
This study explores the effects of incorporating palm oil fuel ash (POFA) and fly ash (FA) as partial cement substitutes on the mechanical properties and characteristics of high-quality mortar, specifically Engineered Cementitious Composites (ECC). ECC mortar was fabricated by milling POFA waste and FA through a top-down method utilizing a ball mill. The resulting material was subjected to tests for slump flow, water absorption, compressive strength, and characterized through XRF, FTIR, SEM/EDX, and XRD analyses. FTIR analysis verified the existence of Si−O and Al−O groups within the composite made of POFA-FA ECC. XRF analysis of FA and POFA showed cementitious properties, with SiO_2+Al_2O_3+Fe_2O_3 exceeding 50% and CaO surpassing 10%. SEM and XRD results indicated minimal cavity formation, suggesting a high compressive strength in the mortar. Particle size distribution analysis revealed prevalent particles in the 1.5×10^{-1} to 2.0×10^{-1} μm range. The compressive strength test after 28 days, incorporating 15% FA and 10% POFA, yielded the highest strength at 59.30 MPa. The water absorption values ranged from 1.25% to 2.67%, indicating that POFA-FA assists in the cement hydration process and also serves as a filler. As a result, the material's density is very high, leading to fewer voids formed, thus reducing the trapped water, which significantly affects the mortar's strength.

Keywords
POFA, Fly Ash, Cementitious Material, Industrial Waste

Received: 27 June 2023, Accepted: 13 November 2023
https://doi.org/10.26554/sti.2024.9.1.59-68

1. INTRODUCTION

The coal sector and the palm oil industry play significant roles in supporting Indonesia's economy. The palm oil production serves multiple functions and has experienced a steady rise in worldwide demand. Additionally, coal-fired power stations are essential for meeting energy requirements across different sectors. The market for both industries has been growing steadily, driven by population growth. However, these industries also generate substantial amounts of byproducts that are often treated as waste (Zawawi et al., 2020; Ghazali et al., 2021; Muthusamy et al., 2020).

One of the essential agro-industries in Southeast Asia and Sub-Saharan Africa is Crude Palm Oil (CPO), which generates palm shells as waste during the processing phase. Indonesia, being one of the world's foremost palm oil suppliers, encounters a direct link between the cultivation of oil palms and the production of palm shells. As palm oil processing increases, so does the amount of palm kernel shells generated. Palm shells hold significant economic value for the palm oil processing industry as they can be utilized as an energy source. When palm shells are used as fuel for power plants, they produce ash, commonly referred to as palm oil fuel ash (POFA). Consequently, the increasing global annual ash production from industries poses a risk of environmental pollution if not managed appropriately (Aldahdooh et al., 2014; Hamada et al., 2020; Khankhaje et al., 2018; Muthusamy et al., 2019; Thomas et al., 2017).

The increase in fuel oil prices has led many industries to switch to using coal as a fuel source, resulting in a continued increase in demand for coal in recent years. Consequently, the production of fly ash (FA) waste from coal-fired power plants has also elevated. Proper management of fly ash waste is essential as it incurs costs for the industry and, if mishandled, can result in environmental pollution and pose health risks to humans. Therefore, it is imperative to implement effective handling practices to mitigate the adverse effects of fly ash (Abdulkareem et al., 2014; Naganathan et al., 2015; Rafieizonooz et al., 2016).

In response to this challenge, several studies have explored the sustainable use of POFA and FA in the construction sec-

tor. As per Sumra et al. (2023), the addition of ground POFA (G-POFA) as a cement substitution in Ordinary Portland Cement (OPC) mortar increased its water absorption due to a more significant pozzolanic reaction. The mortar with 10% G-POFA substitution (G-POFA-10) indicated the highest tolerance to water absorption and sorptivity. Additionally, Jose et al. (2023) found that the water absorption of foamed concrete decreased with an increasing amount of POFA and red gypsum replacement. Alex et al. (2016) further demonstrated that mechanical strength increased with a decrease in fly ash size and a 20 wt% ash replacement in cement. Nonetheless, continuous endeavors are underway to enhance the results by considering a range of factors, including material characteristics, treatment techniques, mix proportions, construction methods, and methodologies. POFA-FA contains abundant cementitious compounds, making it suitable for application as a cementitious material in mortar-engineered cementitious composites (ECC). ECC mortar belongs to the High-Performance Fiber-Reinforced Cementitious Composites (HPFRCC) category, exhibiting high ductility and a moderate fiber fraction (Adesina and Das, 2020; Sherir et al., 2014; Wang and Li, 2007). ECC is a material that can be manufactured by considering microstructure, processing techniques, material properties, and performance. The micromechanical relationship between the mechanical performance of composites and their microstructure occurs (Aldahdooh et al., 2014; de Azevedo et al., 2022; Hamada et al., 2018; Muthusamy et al., 2020). Muthusamy et al. (2021b) conducted a study using a composite of Oil Palm Shell (OPS) and FA to create concrete. The outcomes of compressive strength, flexural strength, and water absorption tests performed over a 28-day period demonstrated that the inclusion of 30% fly ash produced the most favorable results.

Moreover, the adoption of POFA-FA as a construction material is expected to reduce the requirement for and the manufacturing of conventional Portland cement, which has a substantial impact on carbon emissions and the environment. In the pursuit of developing environmentally friendly Portland cement, many studies have explored the potential of waste materials to serve as raw materials and provide sustainable solutions to various global environmental challenges (Hamada et al., 2019; Nath and Sarker, 2014). Therefore, this study introduces the incorporation of POFA-FA into ECC mortar, as it is crucial as a substitute material for cement production. With this explanation in mind, this study aims to assess the mechanical characteristics and attributes of the newly created ECC mortar that utilizes POFA-FA as a key component.

2. EXPERIMENTAL SECTION

2.1 Materials and Instrumental

The POFA utilized was sourced from PT. Tinjowan Oil Palm Plantation (North Sumatra, Indonesia), while FA was obtained from PT. Sinarmas Oleochemical (Medan, North Sumatra, Indonesia). Other materials, such as fine sand and superplasticizer (SP) of the ViscoCrete-3115 N type, were obtained from PT. SIKA, Portland Cement Type I/Ordinary Portland Cement (OPC) from PT. Semen Padang.

The equipment used includes a drill mixer, slump-flow test equipment, cube mold measuring (15×15×15 cm), mix bucket, digital scales, meter, ball mill, compression test machine (ELE INTERNATIONAL, 2000 kN), oven, X-Ray Fluorescence (XRF, PANalytical Minipal 4), Fourier Transform Infra Red (FTIR, Shimadzu IRPrestige-21), X-Ray Diffraction (XRD, OHION), and Scanning Electron Microscopy-Energy Dispersive X-Ray (SEM-EDX Mapping, JEOL JSM-6510LA).

2.2 Methods

2.2.1 ECC Mortar Manufacturing

As indicated in prior research, the ideal proportion for incorporating POFA is between 10-15% (Danish et al., 2023), and for FA in cementitious composites, it should not exceed 15% to avoid any notable impact on workability (Lin et al., 2023). For this reason, POFA-FA and other materials were weighed according to a predetermined mix proportion (Table 1). The mixing process began by combining the superplasticizer and water in a bucket using a drilling machine. Subsequently, the remaining materials, starting with POFA, FA, sand, and type 1 cement, were gradually added. Each addition was accompanied by stirring using a drill machine until the mixture was evenly mixed, after which the next material was added. The mixture in the bucket was continuously stirred until it reached a homogeneous state with good workability, as confirmed by the slump flow test. Following this, the mixed material was transferred to a mold and subjected to a compressive strength test after 28 days (Huseien et al., 2023c).

2.2.2 Sample Preparation for Characterization

This preparation was conducted following the procedures outlined by Satriawan and Awaluddin (2021) and Sumra et al. (2023) with some modifications. The POFA-FA used for characterization was obtained by burning boilers at 800°C. The resulting POFA-FA ash was dried at 110°C for 24 hours, ground using a ball mill for 6 hours at 400 rpm and sieved through a 200-mesh sieve. Subsequently, it was further dried at 500°C for 4 hours and ground using a ball mill for an additional 6 hours at 400 rpm. The refined POFA-FA was characterized using XRF, FTIR, XRD, and SEM-EDX.

2.2.3 Slump-Flow Test

The slump-flow test was performed to assess the ECC mixture's slump flow value and its filling capacity. The Abrams cone was positioned vertically on the base plate and firmly held in place. Within 30 seconds, the ECC mixture was poured into the Abrams cone funnel without any agitation. The Abrams cone was then gradually lifted in a single upward motion of approximately 30 cm, ensuring the mortar flow was undisturbed. Using a stopwatch, the time needed for the ECC mixture to achieve a 500 mm (T500) diameter was recorded immediately after lifting the Abrams cone. The maximum diameter was measured twice (D1 and D2) once the ECC mixture ceased

Table 1. Test Matrices with Various Cementitious Material Compositions

Cementitious Material		Fly Ash (FA) (%)			
		0	5	10	15
Palm Oil Fuel Ash (POFA) (%)	0	0:0	0:5	0:10	0:15
	5	5:0	5:5	5:10	5:15
	10	10:0	10:5	10:10	10:15
	15	15:0	15:5	15:10	15:15

flowing (Akmal et al., 2017). The process of the slump-flow test is displayed in Figure 1.

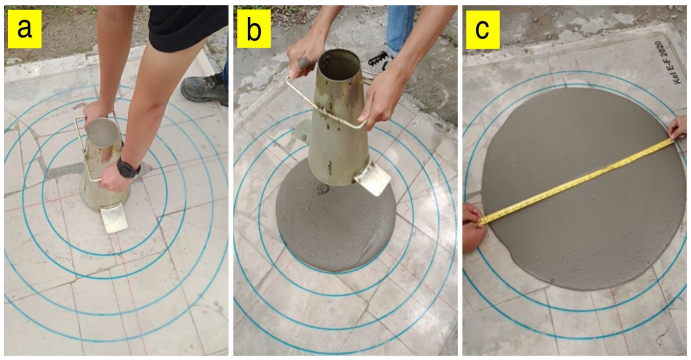

Figure 1. Slump-Flow Test: (a) Placing Abrams Cone, (b) Lifting the Cone after Pouring the ECC Mixture, (c) Diameter Measurement

2.2.4 Water Absorption Test

In this study, the water absorption test for the POFA-FA ECC mortar followed the method proposed by (Huseien et al., 2023b). The ECC mortar specimens were molded into dimensions of 15×15×15 cm, cured for 28 days, and then submerged in water for 24 hours. Subsequently, the POFA-FA ECC mortar samples were weighed after complete submersion in water (Ws). After saturation, the composites were oven-dried for an additional 24 hours at approximately 105°C and then reweighed (Wd). The water absorption values (WA%) for the mixtures were calculated using Equation (1).

$$WA(\%) = \frac{Ws\text{-}Wd}{Wd} \times 100 \quad (1)$$

2.2.5 Compressive Strength Test

The compressive strength of the cured samples was assessed using a compression testing machine with a maximum capacity of 2000 kN. The POFA-FA ECC mortar specimens, aged for 28 days, were placed on the lower plate of the testing device. To accurately capture the failure pattern under uniaxial compression, a loading rate of 0.21 mm/min under displacement control was selected. Compressive strength was estimated by dividing the maximum applied force by the cross-sectional area that resisted the load, following the methodology described by Chub-uppakarn et al. (2023) and Huseien et al. (2023a).

3. RESULTS AND DISCUSSION

3.1 XRF Characterization of POFA and FA

XRF testing was conducted at the Central Laboratory of Minerals and Advanced Materials, State University of Malang, to identify the elements and compounds present in POFA and FA (Naganathan et al., 2015; Nugraha et al., 2007). After the XRF test, the POFA and FA were dried, pulverized in a ball mill, and then sieved through a 200 mesh. Figure 2 displays the appearance of the POFA and FA.

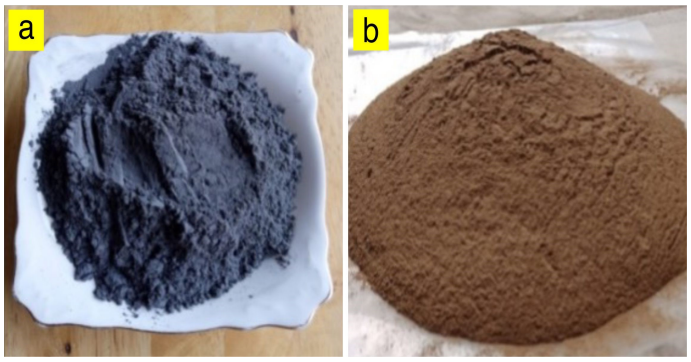

Figure 2. (a) POFA and (b) FA

The findings of the XRF test on POFA and FA are presented in Tables 2 and 3, respectively. Table 2 reveals that POFA has chemical compositions of 48.9% SiO_2, 3.4% Fe_2O_3, and 13.8% CaO, indicating its pozzolanic and cementitious properties (Alsubari et al., 2018). Similarly, Table 3 displays the chemical composition of FA, with SiO_2, Al_2O_3, Fe_2O_3, and CaO constituting 29.3%, 14.0%, 30.9%, and 18.3% respectively. These compositions also contribute to the pozzolanic and cementitious nature of FA.

3.2 EDX and XRD Characterization

Figure 3 illustrates the outcomes of the EDX analysis performed on the POFA-FA ECC mortar. The analysis reveals the existence of different elements and oxides in the materials, with the following composition: C= 21.50%, MgO= 1.03%, Al_2O_3= 14.41%, SiO_2= 36%, SO_3=0.91%, K_2O= 3.10%, CaO= 12.10%, and FeO= 10.95%. According to the EDX data, SiO_2 showed the highest value, primarily due to its elevated silica

Table 2. XRF Characterization Results of POFA

Element	Percentage (%)	Compound	Percentage (%)
Si	32.70	SiO_2	48.90
P	4.90	P_2O_5	6.97
S	2.70	SO_3	4.10
K	31.00	K_2O	20.50
Ca	19.90	CaO	13.80
Ti	0.18	TiO_2	0.15
Mn	1.00	MnO	0.61
Fe	5.17	Fe_2O_3	3.42
Cu	0.26	CuO	0.15
Zn	0.12	ZnO	0.07
Rb	0.76	Rb_2O	0.37
Sr	0.23	SrO	0.12
Mo	0.60	MoO_3	0.50
Ba	0.20	BaO	0.10
Eu	0.20	Eu_2O_3	0.10
Re	0.10	Re_2O_7	0.07

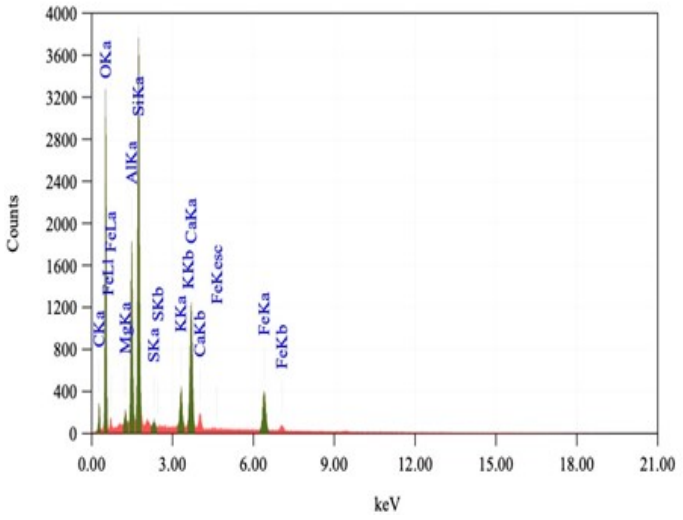

Figure 3. EDX Data of POFA-FA ECC Mortar

Table 3. XRF Characterization Results of FA

Element	Percentage (%)	Compound	Percentage (%)
Al	11.00	Al_2O_3	14.00
Si	19.80	SiO_2	29.30
K	1.50	K_2O	1.14
Ca	21.20	CaO	18.30
Ti	1.57	TiO_2	1.54
V	0.05	V_2O_5	0.05
Cr	0.09	CrO_3	0.07
Mn	0.90	MnO	0.65
Fe	39.6	Fe_2O_3	30.90
Ni	0.04	NiO	0.03
Cu	0.09	CuO	0.06
Zn	0.03	ZnO	0.02
Sr	0.81	SrO	0.48
Mo	2.10	MoO_3	2.10
Ba	0.58	BaO	0.38
Eu	0.59	Eu_2O_3	0.38
Yb	0.04	Yb_2O_3	0.03
Re	0.47	Re_2O_7	0.31

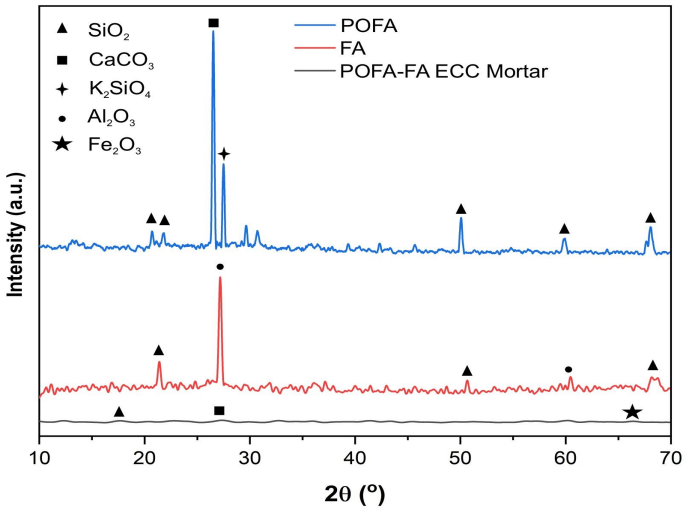

Figure 4. Diffraction Pattern of POFA, FA, and POFA-FA ECC Mortar

(Si) content, which contributes to the improved compressive strength of the mortar (Tosun-Felekoğlu et al., 2017). Much like the EDX analysis, the presence of elements from XRF demonstrated that the raw materials POFA and FA contained the highest amount of silica, with SiO_2+Al_2O_3+Fe_2O_3 exceeding 50%. These findings align with previous studies where the use of POFA in OPC composite manufacturing resulted in SiO_2/Al_2O_3/Fe_2O_3 values ranging from 40% to 60% (Rajak et al., 2023). Therefore, it can be concluded that the composites were successfully created with a high silica content due to the presence of POFA and FA materials, which inherently possess very high silica levels.

X-ray diffraction (XRD) analysis was performed to validate the EDX findings and to characterize the material further. This analysis provided insights into the crystal structure, phase properties, lattice parameters, and crystal grain size, with a particular focus on SiO_2, Fe_2O_3, and Al_2O_3, although silica was the primary component of interest (Ranjbar et al., 2014; Wi et al., 2018). Based on data in Table 4, the XRD analysis results reveal that POFA exhibits a trigonal crystal system (with hexagonal axes), featuring a unit cell with dimensions a= 12.877 Å, and c= 95.244 Å, and a density of 2.42 g/cm^3. By employing crystallography open database (COD) as a tool for phase identification using powder diffraction data, it was possible to identify SiO_2 compounds corresponding to the peaks at a

2θ angle, as depicted in Figure 4. The diffractogram of POFA indicates the presence of SiO_2 peaks at 2θ angles of 20.81°, 21.72°, 50.06°, 59.85°, and 68.10° (Figure 4). Additionally, peaks attributed to $CaCO_3$ and K_2SiO_4 were observed at 2θ angles of 26.52° and 27.50°, respectively.

Moreover, according to the XRD analysis of FA utilizing the data displayed in Table 4, it is evident that the crystal system exhibits hexagonal axes. The unit cell dimensions are identified as a= 4.8120 Å, b= 4.8120 Å, and c= 5.3270 Å, with a corresponding density of 2.80 g/cm^3. According to Figure 4, the diffractogram of FA exhibits SiO_2 peaks at 2θ angles of 21.40°, 50.74°, and 68.66°, while Al_2O_3 peaks are observed at 2θ angles of 27.18° and 60.51°.

The XRD analysis results of POFA-FA ECC mortar indicate an orthorhombic crystal system with unit cell parameters a= 8.314 Å, b= 11.074 Å, and c= 18.296 Å, and a density of 1.49 g/cm^3. Figure 4 displays the SiO_2 peaks at 2θ values of 18.02° and 71.53°. In addition, peaks corresponding to $CaCO_3$ and Fe_2O_3 were observed at 2θ values of 27.14° and 56.21°, respectively.

3.3 FTIR Characterization

The materials POFA, FA, and POFA-FA ECC mortar were subjected to FTIR characterization to identify their functional groups and assess any changes in functional groups following the creation of POFA-FA ECC mortar (Nandiyanto et al., 2019). Figure 5 presents the FTIR results.

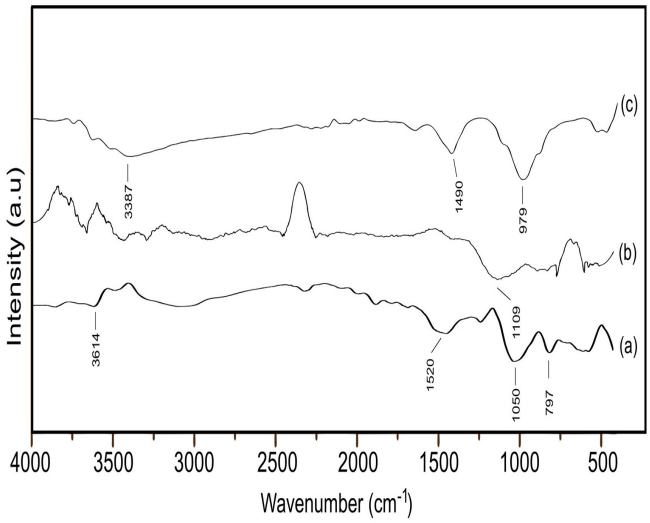

Figure 5. FTIR Spectra of (a) POFA, (b) FA, and (c) POFA-FA ECC Mortar

Based on Figure 5(a), the absorption band at around 3614 cm^{-1} suggests the moderate intensity of the O−H bond from the SiOH group. The peak at approximately 1520 cm^{-1} reveals the asymmetric stretching of the C−O bond (Satriawan and Awaluddin, 2021). Additionally, the band at 1050 cm^{-1} suggests the existence of Si−O bond asymmetric stretching vibration. Furthermore, the peak at 797 cm^{-1} corresponds to the crystalline phase of quartz (Ranjbar et al., 2014; Wi et al., 2018).

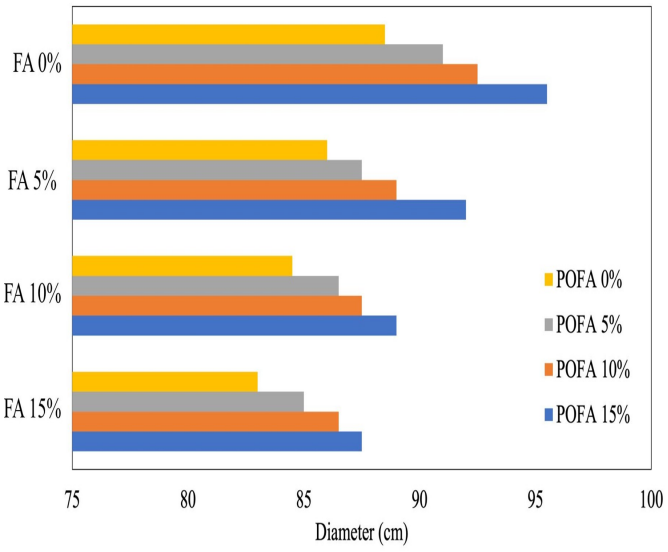

Figure 6. Slump Flow Test Results

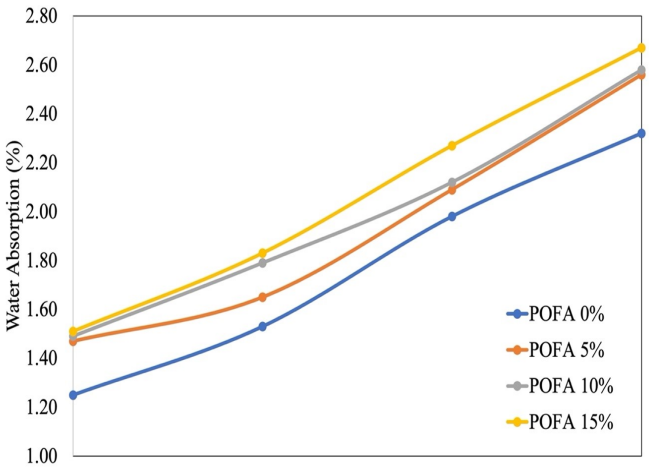

Figure 7. Water Absorption on POFA-FA ECC Mortar

Figure 5(b) demonstrates the stretching vibration of Si−O−Si, which is represented by a peak at 1109 cm^{-1} (Ryu et al., 2013). The FTIR spectra in Figure 5(c) reveal the presence of functional groups in POFA-FA ECC mortar. The wavenumber at 3387 cm^{-1} relates to the O−H stretching vibration from the SiOH group. Furthermore, the wavenumber of the asymmetric stretching C−O bond has shifted from 1520 to 1490 cm^{-1}. The change in the C−O groups is ascribed to the interconnection between the POFA-FA ECC mortar and carbon dioxide throughout the reaction process, resulting in the establishment of bonds between the composite and carbon dioxide (Satriawan and Awaluddin, 2021). Moreover, the peak of 979 cm^{-1} repre-

Table 4. XRD Data Analysis of POFA, FA, and POFA-FA ECC Mortar

Materials	Peak Position 2θ (°)	FWHM B_{size} (°)	D (nm)	hkl	d (Å)
POFA	20.81	0.27	31.26	100	4.1673
	21.72	0.27	31.30	041	2.4335
	26.52	0.26	32.80	10-1	11.0761
	27.50	0.25	34.18	-102	10.8581
	50.06	0.26	35.24	112	4.2109
	59.85	0.39	24.56	271	4.0262
	68.10	0.26	38.54	203	5.5381
FA	21.40	0.45	18.77	111	2.19272
	27.18	0.50	17.08	-122	1.17345
	50.74	0.81	11.34	228	1.09636
	60.51	0.75	12.81	1311	1.42871
	68.66	0.49	20.52	-206	1.64114
POFA-FA ECC Mortar	18.02	16.73	0.50	111	7.17398
	27.14	7.21	1.18	103	4.64035
	56.21	4.64	2.03	413	2.53024
	71.53	6.71	1.52	21-6	2.63930

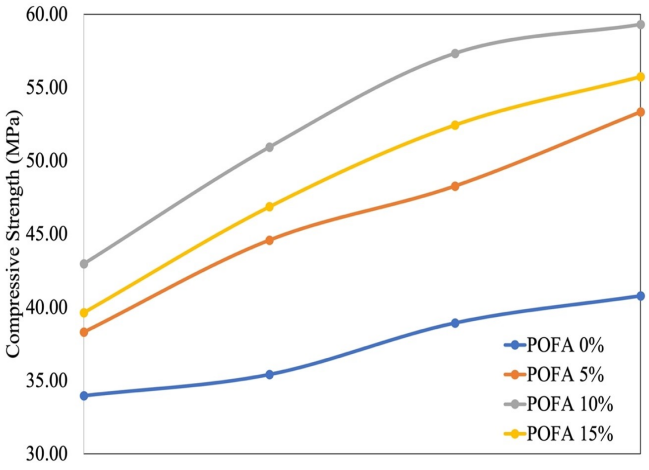

Figure 8. Compressive Strength Test Results of POFA-FA ECC Mortar Aged 28 Days

sents Si−O−Si and Si−O−Al asymmetric stretching vibration (Liu et al., 2016; Ranjbar et al., 2014).

3.4 Slump-Flow Test on POFA-FA ECC Mortar

The ECC mortar's workability was assessed using a slump-flow test, and the results for the POFA-FA ECC mortar are presented in Figure 6. As the percentage of FA in the ECC mortar increased, there was a corresponding rise in the slump-flow value. This indicates that incorporating FA up to 15% in the ECC mixture enhances workability. Conversely, the addition of POFA resulted in a reduction in the slump-flow value (Nugraha et al., 2007). This can be explained by the higher water absorption capacity of POFA in comparison to cement or FA due to its larger granule size. Notably, the test results demonstrated that a POFA:FA mixture with a ratio of 0%:15% exhibited the highest slump-flow value of 95.5 cm. In this research, the specimen with 15% POFA displayed superior slump flow values when contrasted with the other specimens, signifying an enhanced filling capacity of the POFA-FA composite. Additionally, all materials exhibited remarkable stability, with all mixtures achieving a flow time under 5 seconds to attain a 500 mm diameter. Consequently, it can be suggested that the addition of POFA improves the workability of POFA-FA ECC mortar, with greater workability observed at increased POFA content (Sabah et al., 2020; Zaimi et al., 2023).

3.5 Water Absorption of POFA-FA ECC Mortar

Figure 7 demonstrates that the water absorption value ranges from 1.25 to 2.67%. The addition of POFA and FA tends to increase the water absorption value of the mortar. However, it remains significantly below the standard water absorption value of around 5% for concrete (Muthusamy et al., 2020). The water absorption value is directly linked to the size of the pores in mortar or concrete. Excess water in the mortar evaporates, leading to the formation of cavities. When the mortar is soaked or exposed to water, these cavities become filled with water. The strength of mortar or concrete decreases with an increase in the number of pores (Muthusamy et al., 2021a).

According to Ayub et al. (2023), POFA has a pore volume of 0.011 cm^3/g, which can increase up to 0.88 cm^3/g when activated with KOH. Meanwhile, POFA-modified cementitious composites will exhibit a larger pore volume as the amount of POFA increases (> 0.9 cm^3/g). This is because the pore volume of POFA is greater than that of cement. Therefore, optimizing the use of POFA in cement should be carefully considered to ensure that water absorption remains below 5% (Golewski, 2023; Tasnim et al., 2020; Zaimi et al., 2023).

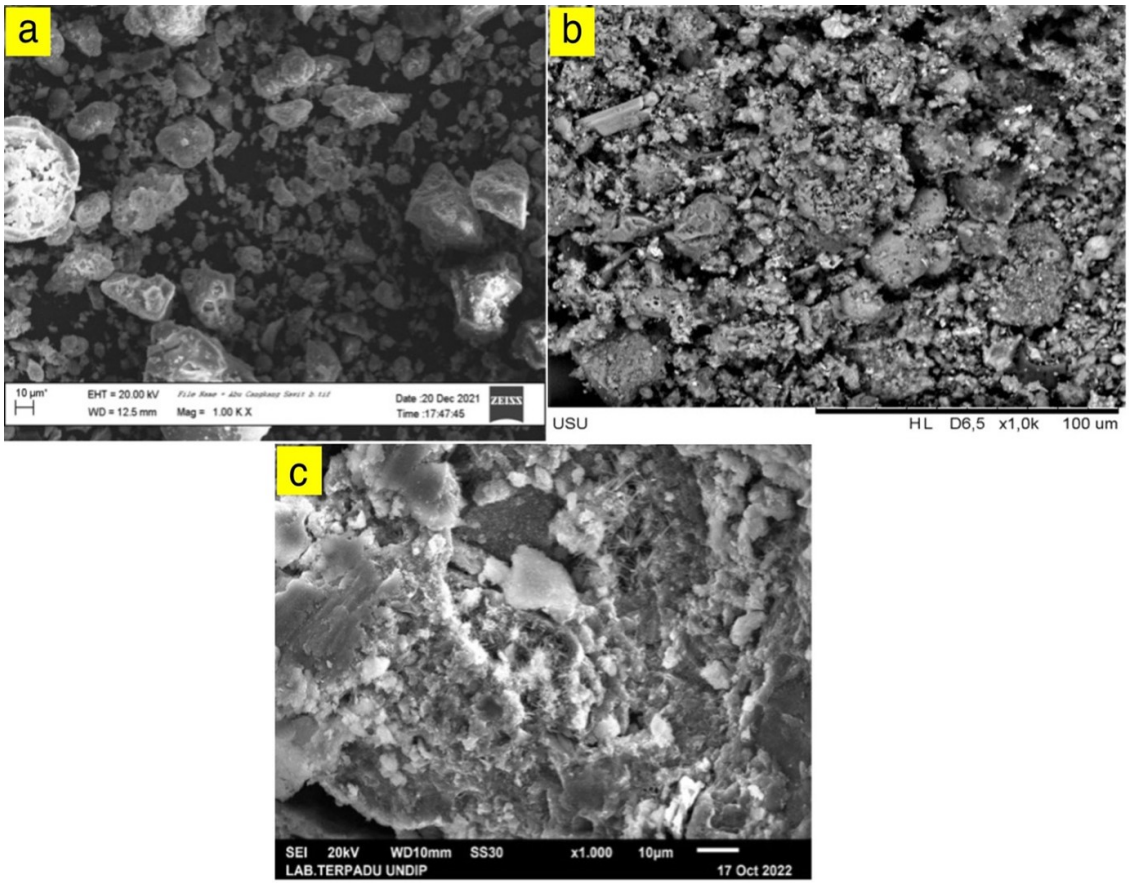

Figure 9. Surface Morphological of (a) POFA, (b) FA, and (c) POFA-FA ECC Mortar at a Magnification of 1000×

3.6 Compressive Strength Measurements

The strength testing in this study was performed using only compressive strength. According to Golewski (2023), the strength of composites can be represented by compressive strength testing, although additional tests such as tensile strength, flexural strength, or others can be added. The trend in the findings of compressive strength testing generally reflects the same trend in other strength tests, such as tensile strength.

The compressive strength results of POFA-FA ECC mortar after 28 days are shown in Figure 8. The inclusion of FA and POFA results in an rise in compressive strength. Nonetheless, a reduction in strength is observed when POFA is added at a 15% ratio. This suggests that adding excessive POFA with a constant cement mass results in an excess of filler that is challenging to bind with cement as a matrix. Additionally, achieving the desired reaction from cementitious materials becomes difficult if the cement mass is not proportional to the cementitious material that will react with cement (Chousidis et al., 2015; Hossain et al., 2016; Ranjbar et al., 2014; Ting et al., 2020). The highest compressive strength (59.30 MPa) was obtained with a POFA:FA ratio of 10%:15%. Generally, the presence of SiO_2, Al_2O_3, Fe_2O_3, and CaO in FA and POFA influences the crucial stages of the cement hydration process, resulting in increased compressive strength in FA-POFA ECC mortar (Chousidis et al., 2015; Hossain et al., 2016).

3.7 SEM Morphology

The morphology of POFA, FA, and FA-POFA ECC mortar was examined through SEM analysis (Liu et al., 2016; Ting et al., 2020. Particle size distribution data were also obtained using SEM. Figure 9(a) shows that POFA exhibits an angular and irregular shape, characterized by granular clumps. The particle size of POFA predominantly falls within the range of 5-15 μm (Figure 10(a)). This indicates a high proportion of extremely fine particles in POFA, potentially impacting the reactivity and workability of the ECC mortar. Conversely, FA (Figure 9(b)) appears as granules with varying shapes. The particle size distribution of FA, displayed in Figure 10(b), is mostly homogeneous at 4 μm, with only a small fraction exhibiting heterogeneity due to agglomerates. Similar to POFA, this morphology influences the reactivity of the ECC mortar.

Meanwhile, Figure 9(c) of POFA-FA ECC mortar reveals the presence of gray color resulting from a lump of FA and black color due to the mixture process, resulting in cavity formation. This SEM image indicates the formation of a few cavities that could potentially impact the mechanical properties of the material. The presence of these cavities within the mortar results in a decrease in mechanical strength, thereby increasing the

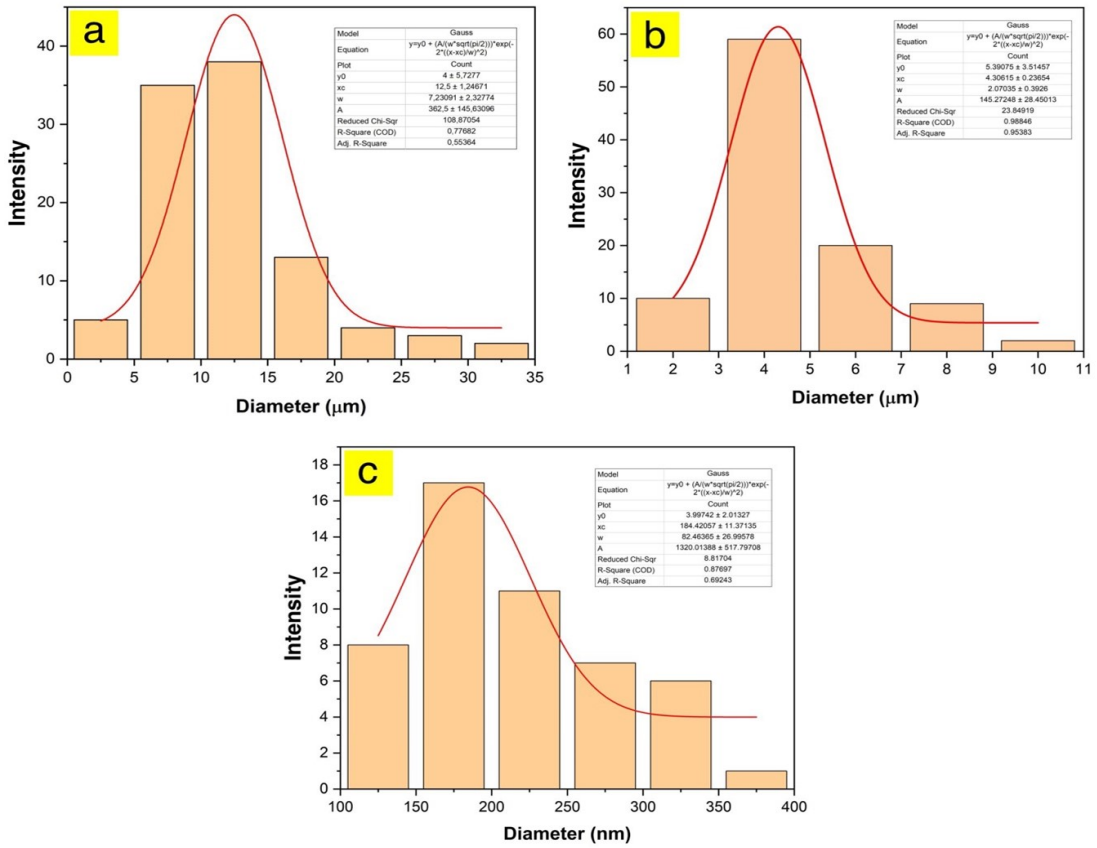

Figure 10. Particle Size Distribution of (a) POFA, (b) FA, and (c) POFA-FA ECC Mortar

susceptibility to cracks or fractures (Siad et al., 2015). Furthermore, the particle size distribution of the manufactured material predominantly falls within the range of 1.5×10^{-1} to 2.0×10^{-1} μm, as shown in Figure 10(c).

4. CONCLUSION

The XRF analysis of FA and POFA indicated that they possess cementitious properties, as evidenced by the presence of SiO_2+Al_2O_3+Fe_2O_3>50% and CaO>10%. This suggests their potential contribution to the cement hydration binding process. The changes in functional groups observed in the cement materials after being incorporated into ECC mortar further validate this effect. The study demonstrates a direct relationship between the incorporation of FA and POFA and the compressive strength of ECC mortar, with the optimal POFA:FA composition of 10%:15% resulting in a strength of 59.30 MPa. SEM analysis was employed to evaluate the surface morphology and particle size distribution of the POFA-FA ECC mortar. The SEM results indicate minimal cavity formation, indicating a high compressive strength of the resulting mortar. Particle size distribution analysis revealed the dominance of particles ranging from 1.5×10^{-1} to 2.0×10^{-1} μm. XRD and EDX analysis confirmed the Si abundance, which contributes to the compressive strength of the POFA-FA ECC mortar. Consequently, the utilization of POFA and FA waste as substitutes for cement presents an effective solution for managing industrial waste from POFA, FA, and Portland cement.

5. ACKNOWLEDGMENT

The authors thank the Ministry of Research, Technology, and Higher Education of the Republic of Indonesia for their financial support provided through the 2019 BPPDN scholarship, under grant number B/67/D.D3/KD.02.00/2019.

REFERENCES

Abdulkareem, O. A., A. M. Al Bakri, H. Kamarudin, I. K. Nizar, and A. S. Ala'eddin (2014). Effects of Elevated Temperatures on the Thermal Behavior and Mechanical Performance of Fly Ash Geopolymer Paste, Mortar and Lightweight Concrete. *Construction and Building Materials*, **50**; 377–387

Adesina, A. and S. Das (2020). Mechanical Performance of Engineered Cementitious Composite Incorporating Glass As Aggregates. *Journal of Cleaner Production*, **260**; 121113

Akmal, A. M. N., K. Muthusamy, F. M. Yahaya, H. M. Hanafi, and Z. N. Azzimah (2017). Utilization of Fly Ash As Partial Sand Replacement in Oil Palm Shell Lightweight Aggregate

Concrete. In *IOP Conference Series: Materials Science and Engineering*, volume 271. IOP Publishing, page 012003

Aldahdooh, M., N. M. Bunnori, and M. M. Johari (2014). Influence of Palm Oil Fuel Ash on Ultimate Flexural and Uniaxial Tensile Strength of Green Ultra-high Performance Fiber Reinforced Cementitious Composites. *Materials & Design*, **54**; 694–701

Alex, J., J. Dhanalakshmi, and B. Ambedkar (2016). Experimental Investigation on Rice Husk Ash As Cement Replacement on Concrete Production. *Construction and Building Materials*, **127**; 353–362

Alsubari, B., P. Shafigh, Z. Ibrahim, and M. Z. Jumaat (2018). Heat-treated Palm Oil Fuel Ash As an Effective Supplementary Cementitious Material Originating from Agriculture Waste. *Construction and Building Materials*, **167**; 44–54

Ayub, M., M. H. D. Othman, M. Z. M. Yusop, I. U. Khan, Z. S. Tai, and S. K. Hubadillah (2023). Optimized Single-step Synthesis of Graphene-based Carbon Nanosheets from Palm Oil Fuel Ash. *Materials Chemistry and Physics*, **296**; 127202

Chousidis, N., E. Rakanta, I. Ioannou, and G. Batis (2015). Mechanical Properties and Durability Performance of Reinforced Concrete Containing Fly Ash. *Construction and Building Materials*, **101**; 810–817

Chub-uppakarn, T., T. Chompoorat, T. Thepumong, W. Sae Long, A. Khamplod, and S. Chaiprapat (2023). Influence of Partial Substitution of Metakaolin by Palm Oil Fuel Ash and Alumina Waste Ash on Compressive Strength and Microstructure in Metakaolin-based Geopolymer Mortar. *Case Studies in Construction Materials*, **19**; e02519

Danish, A., O. Karadag, T. Bilir, and T. Ozbakkaloglu (2023). Valorization of Biomass Ashes in the Production of Cementitious Composites: A Comprehensive Review of Properties and Performance. *Construction and Building Materials*, **405**; 133244

de Azevedo, A. R., M. Amin, M. Hadzima Nyarko, I. S. Agwa, A. M. Zeyad, B. A. Tayeh, and A. Adesina (2022). Possibilities for the Application of Agro-industrial Wastes in Cementitious Materials: A Brief Review of the Brazilian Perspective. *Cleaner Materials*, **3**; 100040

Ghazali, N., K. Muthusamy, R. Embong, I. A. Rahim, N. M. Razali, F. Yahaya, N. Ariffin, and S. W. Ahmad (2021). Effect of Fly Ash As Partial Cement Replacement on Workability and Compressive Strength of Palm Oil Clinker Lightweight Concrete. *Conference Series: Earth and Environmental Science*, **682**(1); 012038

Golewski, G. L. (2023). Assessing of Water Absorption on Concrete Composites Containing Fly Ash up to 30% in Regards to Structures Completely Immersed in Water. *Case Studies in Construction Materials*, **19**; e02337

Hamada, H. M., A. Alya'a, F. M. Yahaya, K. Muthusamy, B. A. Tayeh, and A. M. Humada (2020). Effect of High-volume Ultrafine Palm Oil Fuel Ash on the Engineering and Transport Properties of Concrete. *Case Studies in Construction Materials*, **12**; e00318

Hamada, H. M., G. A. Jokhio, F. M. Yahaya, A. M. Humada, and Y. Gul (2018). The Present State of the Use of Palm Oil Fuel Ash (POFA) in Concrete. *Construction and Building Materials*, **175**; 26–40

Hamada, H. M., F. M. Yahaya, K. Muthusamy, G. A. Jokhio, and A. M. Humada (2019). Fresh and Hardened Properties of Palm Oil Clinker Lightweight Aggregate Concrete Incorporating Nano-palm Oil Fuel Ash. *Construction and Building Materials*, **214**; 344–354

Hossain, M., M. Karim, M. Hasan, M. Hossain, and M. Zain (2016). Durability of Mortar and Concrete Made up of Pozzolans As a Partial Replacement of Cement: A Review. *Construction and building materials*, **116**; 128–140

Huseien, G. F., Z. J. Hussein, Z. Kubba, B. Mikhail Nikolaevich, and J. Mirza (2023a). Improved Bond Strength Performance of Geopolymer Mortars: Role of High Volume Ground Blast Furnace Slag, Fly Ash, and Palm Oil Fuel Ash Incorporation. *Minerals*, **13**(8); 1096

Huseien, G. F., M. Khamehchi, Z. Kubba, O. Benjeddou, and M. J. Mahmoodi (2023b). Freeze-thaw Cycle and Abrasion Resistance of Alkali-activated FA and PPFA-based Mortars: Role of High Volume Gbfs Incorporation. *Heliyon*, **9**(7); e17672

Huseien, G. F., Z. Kubba, and S. K. Ghoshal (2023c). Engineering Attributes of Ternary Geopolymer Mortars Containing High Volumes of Palm Oil Fuel Ash: Impact of Elevated Temperature Exposure. *Fire*, **6**(9); 340

Jose, S. K., S. Anagha, B. Meera, T. Antony, and R. Reenu (2023). Foamed Concrete using Red Gypsum and Palm Oil Fuel Ash: A Sustainable Building Material. *E3S Web of Conferences*, **405**; 03023

Khankhaje, E., M. Rafieizonooz, M. R. Salim, R. Khan, J. Mirza, H. C. Siong, et al. (2018). Sustainable Clean Pervious Concrete Pavement Production Incorporating Palm Oil Fuel Ash As Cement Replacement. *Journal of Cleaner Production*, **172**; 1476–1485

Lin, Y., U. J. Alengaram, and Z. Ibrahim (2023). Effect of Treated and Untreated Rice Husk Ash, Palm Oil Fuel Ash, and Sugarcane Bagasse Ash on the Mechanical, Durability, and Microstructure Characteristics of Blended Concrete–a Comprehensive Review. *Journal of Building Engineering*, **78**; 107500

Liu, M. Y. J., U. J. Alengaram, M. Santhanam, M. Z. Jumaat, and K. H. Mo (2016). Microstructural Investigations of Palm Oil Fuel Ash and Fly Ash Based Binders in Lightweight Aggregate Foamed Geopolymer Concrete. *Construction and Building Materials*, **120**; 112–122

Muthusamy, K., A. M. A. Budiea, N. W. Azhar, M. S. Jaafar, S. M. S. Mohsin, N. F. Arifin, and F. M. Yahaya (2021a). Durability Properties of Oil Palm Shell Lightweight Aggregate Concrete Containing Fly Ash As Partial Cement Replacement. *Materials Today: Proceedings*, **41**; 56–60

Muthusamy, K., A. M. A. Budiea, S. M. S. Mohsin, N. S. M. Zam, and N. E. A. Nadzri (2021b). Properties of Fly Ash Cement Brick Containing Palm Oil Clinker As Fine Aggregate

Replacement. *Materials Today: Proceedings*, **46**; 1652–1656
Muthusamy, K., M. S. Jaafar, N. W. Azhar, N. Zamri, N. Samsuddin, A. M. A. Budiea, and M. F. M. Jaafar (2020). Properties of Oil Palm Shell Lightweight Aggregate Concrete Containing Fly Ash As Partial Cement Replacement. In *IOP Conference Series: Materials Science and Engineering*, volume 849. IOP Publishing, page 012048
Muthusamy, K., J. Mirza, N. A. Zamri, M. W. Hussin, A. P. A. Majeed, A. Kusbiantoro, and A. M. A. Budiea (2019). Properties of High Strength Palm Oil Clinker Lightweight Concrete Containing Palm Oil Fuel Ash in Tropical Climate. *Construction and Building Materials*, **199**; 163–177
Naganathan, S., A. Y. O. Mohamed, and K. N. Mustapha (2015). Performance of Bricks Made Using Fly Ash and Bottom Ash. *Construction and Building Materials*, **96**; 576–580
Nandiyanto, A. B. D., R. Oktiani, and R. Ragadhita (2019). How to Read and Interpret FTIR Spectroscope of Organic Material. *Indonesian Journal of Science and Technology*, **4**(1); 97–118
Nath, P. and P. K. Sarker (2014). Effect of GGBFS on Setting, Workability and Early Strength Properties of Fly Ash Geopolymer Concrete Cured in Ambient Condition. *Construction and Building Materials*, **66**; 163–171
Nugraha, P. et al. (2007). *Teknologi Beton; Dari Material, Pembuatan, Ke Beton Kinerja Tinggi*. Yogyakarta: Andi (In Indonesia)
Rafieizonooz, M., J. Mirza, M. R. Salim, M. W. Hussin, and E. Khankhaje (2016). Investigation of Coal Bottom Ash and Fly Ash in Concrete As Replacement for Sand and Cement. *Construction and Building Materials*, **116**; 15–24
Rajak, M. A. A., Z. A. Majid, and M. Ismail (2023). Hydration of Hardened Cement Paste Incorporates Nano-Palm Oil Fuel Ash at Later Age: The Microstructure Studies. *matrix*, **6**; 7
Ranjbar, N., M. Mehrali, U. J. Alengaram, H. S. C. Metselaar, and M. Z. Jumaat (2014). Compressive Strength and Microstructural Analysis of Fly Ash/palm Oil Fuel Ash Based Geopolymer Mortar under Elevated Temperatures. *Construction and Building Materials*, **65**; 114–121
Ryu, G. S., Y. B. Lee, K. T. Koh, and Y. S. Chung (2013). The Mechanical Properties of Fly Ash-Based Geopolymer Concrete with Alkaline Activators. *Construction and Building Materials*, **47**; 409–418
Sabah, S. A., Z. Zainul, S. Hashim, and M. M. Johari (2020). The Influence of Palm Oil Fuel Ash on the Fresh Properties of Green Self-compacting Concrete. In *IOP Conference Series: Materials Science and Engineering*, volume 849. IOP Publishing, page 012066
Satriawan, A. and A. Awaluddin (2021). The Utilization Silica from Oil Fly Ash as a Raw material for Paper Filler. In *Journal of Physics: Conference Series*, volume 2049. IOP Publishing, page 012062
Sherir, M. A., K. M. Hossain, and M. Lachemi (2014). Fracture Energy Characteristics of Engineered Cementitious Composites Incorporating Different Aggregates. In *CSCE 2014 4th International Structural Specialty Conference*
Siad, H., A. Alyousif, O. K. Keskin, S. B. Keskin, M. Lachemi, M. Sahmaran, and K. M. A. Hossain (2015). Influence of Limestone Powder on Mechanical, Physical and Self-healing Behavior of Engineered Cementitious Composites. *Construction and Building Materials*, **99**; 1–10
Sumra, Y., S. Payam, A. C. Iftikhar, M. Rizwan, A. K. Tanveer, A. Belal, and G. Mustabshirha (2023). Chemical and Thermal Characterization of Cement Mortar Containing Ground Palm Oil Fuel Ash as a Partial Cement Replacement. *Journal of Wuhan University of Technology-Mater. Sci. Ed.*, **38**(3); 575–581
Tasnim, S., Y. Du, M. E. Rahman, R. B. Ahmadi, and S. I. Doh (2020). Effect of Using Palm Oil Fuel Ash on the Durability of Cement Paste in Ammonium Nitrate Solution. *Construction and Building Materials*, **257**; 119597
Thomas, B. S., S. Kumar, and H. S. Arel (2017). Sustainable Concrete Containing Palm Oil Fuel Ash As a Supplementary Cementitious Material–a Review. *Renewable and Sustainable Energy Reviews*, **80**; 550–561
Ting, T. Z. H., M. E. Rahman, and H. H. Lau (2020). Sustainable Lightweight Self-compacting Concrete Using Oil Palm Shell and Fly Ash. *Construction and Building Materials*, **264**; 120590
Tosun-Felekoğlu, K., E. Gödek, M. Keskinateş, and B. Felekoğlu (2017). Utilization and Selection of Proper Fly Ash in Cost Effective Green Htpp-ecc Design. *Journal of Cleaner Production*, **149**; 557–568
Wang, S. and V. C. Li (2007). Engineered Cementitious Composites with High-volume Fly Ash. *ACI Materials Journal*, **104**(3); 233
Wi, K., H.-S. Lee, S. Lim, H. Song, M. W. Hussin, and M. A. Ismail (2018). Use of an Agricultural By-product, Nano Sized Palm Oil Fuel Ash As a Supplementary Cementitious Material. *Construction and Building Materials*, **183**; 139–149
Zaimi, S. A., M. N. Muhd Sidek, N. H. Hashim, H. Mohd Saman, R. Putra Jaya, and N. A. Marzuki (2023). Potential of Palm Oil Fuel Ash as a Partial Replacement of Fine Aggregates for Improved Fresh and Hardened Mortar Performance. *Advances in Civil Engineering*, **2023**
Zawawi, M. N. A. A., K. Muthusamy, A. P. A. Majeed, R. M. Musa, and A. M. A. Budiea (2020). Mechanical Properties of Oil Palm Waste Lightweight Aggregate Concrete with Fly Ash As Fine Aggregate Replacement. *Journal of Building Engineering*, **27**; 100924

